Applied Physics B (2018) 124:171
https://doi.org/10.1007/s00340-018-7033-7

Applied Physics B
Lasers and Optics

Modeling and measuring the quality factor of whispering gallery mode resonators

Anatoliy A. Savchenkov[1] · Simone Borri[2,3] · Mario Siciliani de Cumis[2,4] · Andrey B. Matsko[1] · Paolo De Natale[2,3] · Lute Maleki[1]

Received: 15 January 2018 / Accepted: 23 July 2018 / Published online: 6 August 2018

Abstract
In this paper, we study an experimental method of evaluation of efficiency of an evanescent field coupling of light to a dielectric whispering gallery mode resonator. We show that change of the relative contrast of the observable optical resonance provides an accurate and complete information about the loaded as well as unloaded bandwidth of the resonator mode. We introduce a model of the coupling that allows for an interpolation of the resonator quality factor using experimental data taken without usage of a frequency tunable narrow line laser, a fast photodiode, as well as a frequency reference. The method is also immune to imperfect geometrical mode matching frequently occurring in a realistic system. We validate this model experimentally at both 1.5 and 4.5 μm.

1 Introduction

Characterization of a linear optical microresonator is a trivial task if one has available a tunable source of light, with linewidth much narrower than the bandwidth of the resonator, and a frequency reference, to quantify the frequency shift of the source emission. By scanning the light frequency simultaneously through the resonator mode of interest and through a reference cavity, for example, one can measure the frequency bandwidth of the resonator mode [1]. Many other methods of bandwidth measurement exist. Some of them call for availability of either a fast modulation of the probe light source (e.g., phase modulated light technique) [2] or a fast photodiode (e.g., ring down technique [3–6]). Nonetheless, tunable optical sources and reference cavities are not always available, and an accurate measurement of the quality factor of the modes of a linear cavity becomes complex if made outside of a conventional wavelength domain. This is the case of the IR frequency domain, since modulatable narrow line IR sources, IR phase modulators, and fast IR detectors are accessible, if existing, in a few well equipped laboratories only. In this paper we describe a method to accurately measure the optical bandwidth of a whispering gallery mode resonator (WGMR) that involves only a slow photodiode and an accurate mechanical stage that allows to change the spatial gap between the WGMRs surface and the surface of an evanescent field coupler.

WGMRs are monolithic resonators fabricated from optically transparent materials, such as glass, fused silica, and optical crystals [7–10]. Light is confined in the resonator modes due to total internal reflection and, as result, the finesses of these resonators can be as high as 10^7 [4, 11, 12], larger than other types of resonators. WGMRs are able to sustain a high finesse and quality (Q-) factor through a broad wavelength range, which is inaccessible to resonators involving high-quality mirrors. Evanescent field couplers are utilized to access the modes of the resonators. By adjusting the distance between the couplers and the resonator surface one is able to utilize the same coupler at any desirable wavelength where WGMs are supported. The proposed WGMR spectroscopy technique enables qualification of the

This article is part of the topical collection "Mid-infrared and THz Laser Sources and Applications" guest edited by Wei Ren, Paolo De Natale and Gerard Wysocki.

✉ Simone Borri
simone.borri@ino.cnr.it

[1] OEwaves Inc., 465 N. Halstead Street, Suite 140, Pasadena, CA 91107, USA

[2] CNR-INO, Istituto Nazionale di Ottica, Largo E. Fermi 6, 50125 Firenze, FI, Italy

[3] INFN, Istituto Nazionale di Fisica Nucleare, Sez. di Firenze, Via Nello Carrara 1, 50019 Sesto Fiorentino, Italy

[4] ASI, Agenzia Spaziale Italiana, Contrada Terlecchia s.n.c., 75100 Matera, MT, Italy

resonators through several octaves having in hand relatively narrow line optical sources with limited tunability as well as slow photodiodes.

Coupling efficiency to a WGM resonator can be tuned by modifying the size of the air gap between the resonator and an evanescent field coupler. When the intracavity loss associated with the coupler and intrinsic attenuation match, a phenomenon of critical coupling is observed. In this case all the light entering the resonator is attenuated in it [13]. Variation of the Q-factor of a prism-coupled microsphere with modification of the air gap size was observed experimentally [14]. Control of resonator coupling in a silica microsphere integrated with a fiber taper was achieved via introduction of an external probe attenuator placed at a given distance from the resonator surface [15]. Nearly ideal coupling efficiency of a microsphere and a fiber taper was reported in [16]. In that research control of a tapered-fiber coupler–resonator distance was demonstrated to study coupling loss versus intrinsic loss in both mode-matched coupling condition and mode-mismatched coupling condition. In this paper we report on the development of an experimental technique for measuring loading efficiency of a microresonator integrated with a coupling prism and utilize the method for validation of the analytical expression for the coupling efficiency. Unlike previous studies proving in-principle existence of the critical coupling conditions for the microcavity, here we validate the analytical formula suitable for evaluation of the coupling efficiency.

The method proposed here addresses multiple challenges of microresonator spectroscopy. For example, it allows quantifying the loaded bandwidth of a microresonator as a function of the distance between the evanescent field coupler and the resonator surfaces. We confirm that measuring the gap and the wavelength it is possible to predict the loaded Q-factor. A measurement of a WGMR bandwidth is problematic in multimode resonators because of low contrast of the overloaded resonance (if a single coupler is used) and because of the dense mode spectrum (the modes start to overlap in frequency as the loading increases, so the measurement of the bandwidth becomes inaccurate). The proposed method solves the problem. It also allows overcoming the auto-criticality phenomenon occurring when the resonator is not perfectly mode matched with the incoming light, so that light transmitted from the resonator and reflected from the prism, without entering the resonator, interferes destructively and creates an impression that the overloaded resonator is critically coupled.

In what follows we present a theoretical substantiation of the measurement technique of the WGMR bandwidth and verify it experimentally at 1.5 and 4.5 μm. We confirm applicability of the analytical formula [14] describing evanescent field coupling with a spherical WGMR for description of the evanescent field coupling with a spheroidal WGMR. Using experimental data we evaluate the loading coefficient for a spheroidal WGMR and validate the analytical formula used to describe the loading as a function of the air gap between the resonator and the prism surfaces. The analytical formula is used to find how the loading of a resonator changes with the wavelength and the result is confirmed experimentally by measuring resonator Q-factor at both 1550 and 4550 nm using the technique described in the paper as well as the conventional high-resolution spectroscopy methods. We show, using this technique, that a CaF_2 WGMR has approximately 2 MHz bandwidth at 4.5 μm. This value is within the range of recently measured Q values in crystalline WGMRs around this wavelength.

2 Theory

2.1 Mode-matched coupling

Let us consider an arbitrary WGMR coupled to external space with a single evanescent field prism coupler. For any shape of the resonator surface curvature we can describe the half width at the half maximum (HWHM) associated with the loading of the resonator modes as

$$\gamma_c = \gamma_{c0} e^{-d/d_0}, \tag{1}$$

where γ_c is the coupling-related HWHM, γ_{c0} is the half width at the half maximum at zero spatial gap, $d = 0$; d is the distance between the surfaces of the resonator and the prism, d_0 is the evanescent field parameter defined as

$$d_0 = \frac{\lambda}{4\pi\sqrt{n_r^2 - 1}}, \tag{2}$$

where λ is the optical wavelength, n_r is the refractive index of the resonator. This parameter does not depend on the shape of the resonator.

The amplitude transfer function of the resonator in the case of perfect spatial matching of the pump light and the resonator mode can be written in form

$$S_c = \frac{\gamma - \gamma_c - i(\omega - \omega_0)}{\gamma + \gamma_c - i(\omega - \omega_0)}, \tag{3}$$

where ω_0 and ω are the WGM and optical pump frequencies, respectively, γ is the intrinsic HWHM of the WGM resonance related to intrinsic losses in the mode ($\gamma + \gamma_c$ is the loaded HWHM).

In this ideal case the resonant power reflection coefficient for the resonator/prism system is

$$R(\omega = \omega_0, d) = |S_c|^2_{\omega=\omega_0} = \left(\frac{\gamma - \gamma_c}{\gamma + \gamma_c}\right)^2. \tag{4}$$

Equations (1) and (4) are convenient for studying dependence $R(d)$. We introduce the distance d_1 corresponding to the critical coupling of the resonator as $R(d_1) = 0$, so that

$$\frac{\gamma_{c0}}{\gamma} = \mathrm{e}^{d_1/d_0}, \tag{5}$$

and then use expression

$$R(\omega = \omega_0, d) = \left(\frac{1 - \mathrm{e}^{(d_1-d)/d_0}}{1 + \mathrm{e}^{(d_1-d)/d_0}}\right)^2 \tag{6}$$

to fit the experimental points and find d_1. As soon as d_1 is found and d_0 is known a priori we can calculate γ_{c0} and γ.

This result can be easily evaluated experimentally since γ can be directly and accurately measured in the strongly undercoupled mode if the phase modulated light is available, and $\gamma + \gamma_{c0}$ can be measured for the critically coupled mode. The advantage of the technique is that the complexity of the measurement of the loaded quality factor (Eq. 6) is shifted to the measurements performed when the resonator is nearly critically coupled or undercoupled, which is advantageous in the realistic case considered in what follows.

2.2 Mode-mismatched coupling

In a realistic case the pump light and the resonator mode are spatially mismatched, so some light enters the resonator, and some light reflects from the coupling point. The transmitted and reflected light interact at the photodiode creating an interference pattern influenced by the loading of the resonator. Therefore, one may observe a nearly zero transmission with an overcoupled resonator mode. The measured power reflection coefficient in this case can be parameterized as

$$R_\mathrm{m}(\omega, d) = \alpha\left|\sqrt{\zeta}\mathrm{e}^{i\phi_\zeta} + \sqrt{1-\zeta}S_\mathrm{c}\right|^2, \tag{7}$$

where $\alpha \le 1$ is the frequency independent insertion loss (occurring, e.g., due to limited size of the aperture of the photodiode), $\zeta \le 1$ and ϕ_ζ describe the interference between the transmitted and reflected waves (both these parameters depend on d), and S_c is defined by Eq. (3). The power reflection coefficient $R_\mathrm{m}(\omega, d)$ may not coincide by magnitude with power transfer function $|S_\mathrm{c}|^2$ in the case of interference of the spatial or polarization modes [17].

Introducing $\phi_S = \arg S_\mathrm{c}$, we find that $R_\mathrm{m}(\omega) = 0$ for $\cos(\phi_\zeta - \phi_S) = -1$ and $\sqrt{\zeta} = \sqrt{1-\zeta}|S_\mathrm{c}|$. This is the so called auto-criticality condition that shows that the standard idealized analysis of the mode loading may not be applied to a mode-mismatched resonator–coupler configuration. Prediction of the system behavior is hard since parameter ζ depends on d in an unknown way depending on the configuration of a particular system. Usually ζ increases as d decreases, that makes the observation of a trustworthy overloaded regime a hard task. For the case of partially loaded resonator and relatively good mode matching ($\xi \ll 1$, $\gamma \gg \gamma_\mathrm{c}$, $S_\mathrm{c} \sim 1$), we find that

$$R(\omega = \omega_0, d) = \frac{R_\mathrm{m}(\omega = \omega_0, d)}{R_\mathrm{m}(|\omega - \omega_0| \gg \gamma, d)}. \tag{8}$$

In other words, information about the ideal loading dependence on the parameter d can be retrieved from the measurements.

Equation (8) was utilized as the ground to normalize the measured data in Fig. 2a, b as well as Fig. 4, shown in what follows. Indeed, since we used a coupling prism and mode matching was not perfect and since the resonator spectrum contained a multiple number of modes, the power collected on a photodiode was always significantly less than unity. It means that Eq. (6) cannot be used to fit the data directly. Performing normalization in accordance with Eq. (8) we removed the inconsistency and found the loaded and intrinsic bandwidth of the resonator modes.

3 Experiment

3.1 Experimental setup for WGMR loading measurements at 1550 nm

To verify Eq. (4), we created a setup shown in Fig. 1. The whole setup with translation stages, collimators and resonator mount was mounted on a 2.4″ aluminum honeycomb breadboard. The breadboard was installed on a bench with vibrational isolation pads.

A CaF_2 WGM resonator with a 35 GHz free spectral range (FSR), having a 2.2 mm diameter, was fabricated out of a cylindrical preform. The resonator had a prolate spheroidal shape with the ratio of axes equal to approximately 2. To interrogate the resonator modes we used an

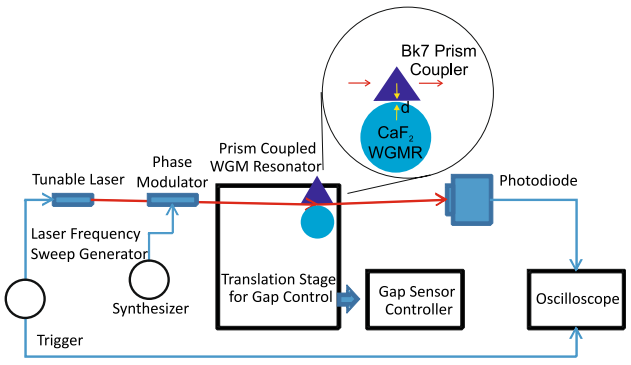

Fig. 1 Setup used to study the dependence of the loaded resonator bandwidth on the air gap, d, between the surface of the resonator and the surface of the prism

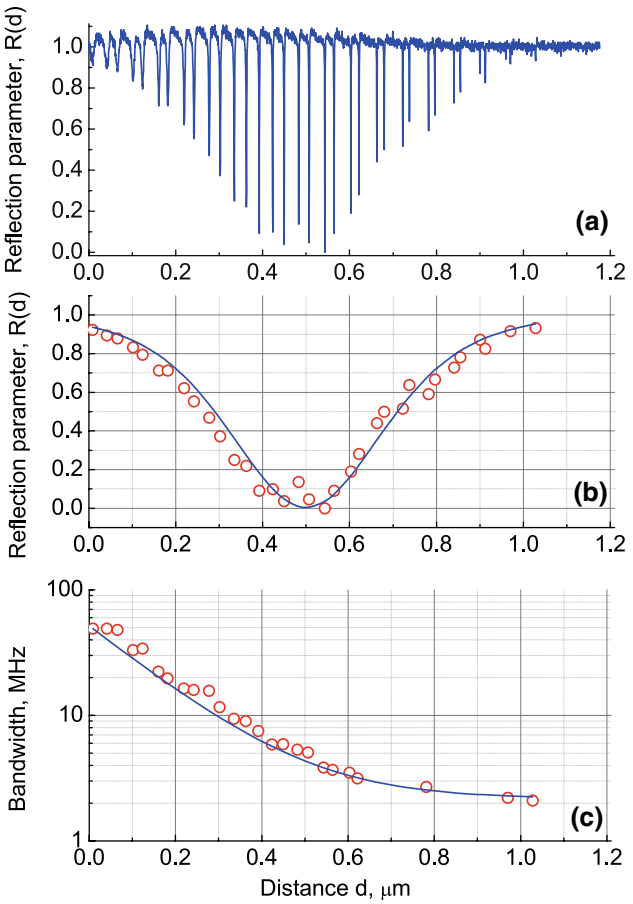

Fig. 2 **a** A set of optical spectra taken in the experiment. The data contain doublets corresponding to forward and backward scans of the laser frequency while the air gap between the prism and the resonator was slowly increasing. The opening speed was constant, but it was not measured. The bandwidth of the mode was measured at the point of critical coupling and it was supposed to be 1.5 MHz. **b** Red circles stand for the minima of the resonances shown in **a**. The blue curve is the fit using Eq. (4). The fit parameters are $d_0 = 0.125\,\mu$m and $d_1 = 0.5\,\mu$m. **c** Measured bandwidth of the mode. When the distance is null the bandwidth value inferred is 46 MHz

evanescent prism coupler made of BK7 glass and having 3 mm height and 57° angles. The prism was antireflection coated for 1550 nm light.

A fiber laser (Koheras) was used to measure the bandwidth of WGMs. The laser had 7 kHz instantaneous linewidth and emitted light at wavelength $\lambda = 1549$ nm. The emission power was kept at the level of 30 mW and then attenuated at the input of the collimator. The high operation power was selected to reduce amplified spontaneous emission noise. The attenuation was used to avoid influence of the nonlinearity of the resonator on the measurement results. Only 3 μW of power entered the resonator. At this power level the observed spectrum did not show any deformation of the resonance curve due to thermal bistability effects.

The reflection $R(d)$ was measured in an experiment performed with the fundamental TE mode family ($\vec{E}||\vec{Z}$) of the resonator. During the measurement, the gap was slowly opening while the frequency of the laser was swept linearly and periodically (a symmetric sawtooth signal) 20 times while the gap opened completely. The sweep rate was about 50 Hz. The laser frequency sweep was produced by a function generator (Agilent 33210A).

The air gap between the prism and the resonator, d, was controlled by a NanoMax-TS Thorlabs translation stage. The gap variations were measured with the help of a Thorlabs APT piezo controller and ultimately calibrated using interference rings observable between the prism surface and the resonator. Piezo sweep was performed by another function generator (Agilent 33210A).

3.2 WGMR spectroscopy results at 1550 nm

The complete experimental data set is shown in Fig. 2a. We used Eq. (4) to fit the minima of the resonance curves of the data set. The fit curve is shown in Fig. 2b. The fitting parameter for the shown curve is $d_1 = 0.5\,\mu$m (the critical coupling corresponds to the minimum of the envelope fitting the minima of the reflection curves). The evanescent field parameter (Eq. 2) is $d_0 = 0.12\,\mu$m for the given laser wavelength and refractive index of CaF_2 at that wavelength ($n_r = 1.426$). The resonator bandwidth dropped exponentially with an increase of the air-gap value (Fig. 2c). The measured bandwidth at $d = 0.54\,\mu$m was approximately 1.5 MHz, while the bandwidth measured for a fully loaded resonator was approximately 100 MHz.

Using ratio d_1/d_0 and Eq. (5) we find $\gamma_{c0}/\gamma = 62$. Since the bandwidth of the critically coupled resonator is equal to 4γ, we find that the loaded bandwidth of the mode is $2\gamma_{c0} = 46$ MHz, as observed in the experiment. Therefore, Eq. (4) is suitable for the description of the resonator loading.

3.3 Validation of the WGMR loading formula

The next question is related to the validation of the analytical formula describing the loaded bandwidth of the resonator mode. There is a formula obtained for TM modes ($\vec{E}\perp\vec{Z}$) of a microsphere [14] (please see Eq. 42 in the reference [1]; please note that the TE_{llq} modes of the microsphere have ($\vec{E}\perp\vec{Z}$) and correspond to TM modes in the planar waveguide description that we adopted here)

$$2\gamma_{\mathrm{TM}\,c0} = \nu_0 \frac{2n_r\sqrt{n_p^2 - n_r^2}}{\pi(n_r^2 - 1)l^{3/2}}, \tag{9}$$

where $\nu_0 = c/\lambda$ is the optical frequency, c is the speed of light in the vacuum, $n_p = 1.5$ is the refractive index of the BK7 prism coupler, $l = 2\pi\nu_0 a n_r/c$ is the mode number, a

is the radius of the resonator. The bandwidth of TM modes is approximately $(n_r^2 - 1)^2$ times smaller as compared with the bandwidth of TE modes because of better confinement of TM modes.

Equation (9) was derived to describe prism coupling with a microsphere resonator and it is useful to verify it for the toroidal resonator we used. Substituting the numbers to Eq. (9) and taking into account the factor n_r^4 we find that the full width at half maximum of the fully loaded WGM is expected to be $2\gamma_{\mathrm{TE}\ c0} = 167$ MHz. This prediction exceeds the experimentally measured value by 3.6 times. Therefore second member of Eq. 9 has to be divided by numerical factor 3.6 to predict the effective bandwidth of the TE resonator modes for our resonator with toroidal geometry. It is important to stress here that the numerical factor 3.6 shows the difference of the analytical formula derived for a microsphere coupled to a planar waveguide and measured numbers for the toroidal resonator.

For a birefringent resonator it is reasonable to introduce ordinary, n_o, and extraordinary, n_e, refractive indexes, instead of n_r. The analytical formulas for the loaded bandwidth become

$$2\gamma_{\mathrm{TM}\ c0} = \nu_0 \frac{2n_o\sqrt{n_p^2 - n_o^2}}{3.6\pi(n_o^2 - 1)l_{TM}^{3/2}}, \tag{10}$$

$$2\gamma_{\mathrm{TE}\ c0} = \nu_0 \frac{2n_e(n_e^2 - 1)\sqrt{n_p^2 - n_e^2}}{3.6\pi l_{\mathrm{TE}}^{3/2}}. \tag{11}$$

3.4 WGMR Q-factor in the mid-IR

The measurement of the Q-factor via the loading technique allows characterization of the WGMR bandwidth at mid-IR frequencies when other standard techniques are not readily available because of the lack of suitable components (e.g., broadband phase modulators, tunable sources, reference cavities, fast enough photodiodes). To demonstrate the validity of the technique we built a packaged WGMR and studied its Q-factor using the loading technique and also using mid-IR frequency references (an etalon and a Doppler-broadened molecular transition). The measurements using loading technique were performed in California, while the spectroscopy using mid-IR frequency references was performed in Italy. The resonator integrated with the couplers was transferred from California to Italy with no damage observed.

The resonator was fabricated out of a cylindrical CaF_2 preform via mechanical polishing. It had approximately 3.6 mm in diameter, corresponding to 18.9 GHz free spectral range at 4.5 μm wavelength. The resonator was mounted inside a custom-made semi-hermetic housing, one wall of which was made of sapphire to provide evanescent field coupling with the resonator modes (Fig. 3). The housing was utilized to reduce both ambient thermal and mechanical fluctuations and also to protect the resonator surface from humidity and dust.

The resonator housing was engineered to allow tuning loading of the resonator modes by changing the temperature of the housing. The temperature change also resulted in a shift of the resonator spectrum at about 0.85 GHz/K rate. To avoid the evanescent field coupler touching the resonator surface, the air gap size was increasing while lowering the temperature towards room temperature.

Two well balanced evanescent field couplers were used in this experiment and transmission through the resonator mode was recorded instead of the reflection from the resonator. The resonant power transmission is described by the formula

$$T(\omega = \omega_0, d) = \left(\frac{2\gamma_c}{2\gamma_c + \gamma}\right)^2, \tag{12}$$

where we assume that each coupling prism broadens the resonance by the same amount, γ_c.

Using a quantum cascade laser (QCL) at 4.5 μm we performed the measurement of $T(\omega = \omega_0, d)$ (Fig. 4) which shows that the FWHM determined by the intrinsic attenuation is given by $2\gamma = \gamma_{c0}/25$. The loaded HWHM bandwidth for the resonator mode is $\gamma_{c0} = 50$ MHz for the given parameters of the resonator. It means that the intrinsic FWHM is approximately 2 MHz. The loaded bandwidth γ_{c0} was found using Eq. 10. In this measurement, we tuned the laser frequency using laser current to measure the loaded Q. Since we did not have a mid-IR phase modulator and fast

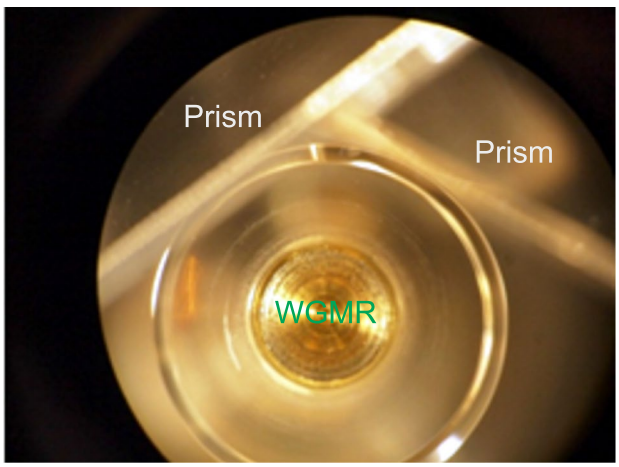

Fig. 3 CaF_2 WGMR integrated in the package. Coupling with input–output sapphire prism couplers is visible at the figure

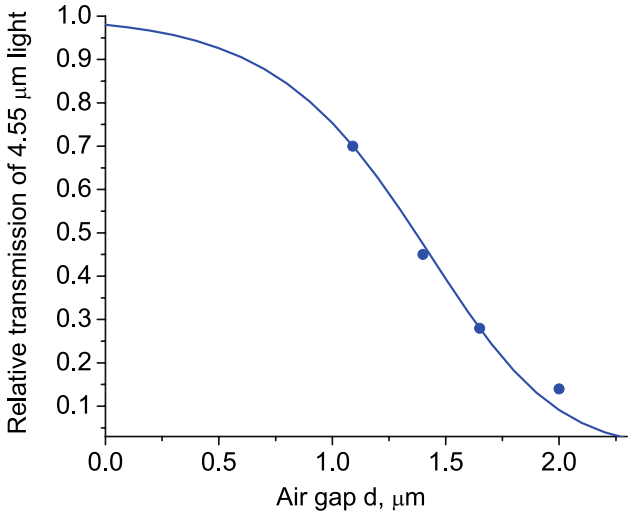

Fig. 4 Dependence of the mid-IR transmission through the CaF_2 WGMR integrated in the package shown in Fig. 3 versus the air gap d. Points correspond to the experimental measurements, while the curve is plotted using Eq. (12) for $2\gamma_{c0}/\gamma = 100$. The figure includes only four data points, and they are all at the over-coupling side. We used a free running quantum cascade laser with a few MHz linewidth. Only overloaded Q-factor can be measured accurately in this way, since the mode bandwidth should exceed the laser linewidth significantly. The fitting using four, one-sided data points introduce fitting error less than 20%. The subsequent measurements performed using a narrow line laser confirmed our measurement result

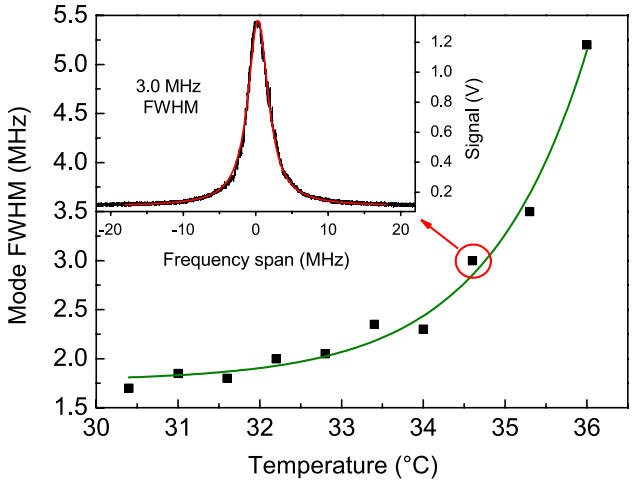

Fig. 5 Dependence of the FWHM of a CaF2 WGM resonator on the temperature of the mounting structure used to tune the spatial gap d between the resonator and the sapphire prism coupler. The corresponding gap size d was not detected during the measurement since the resonator was integrated in a package

photodiode we were not able to measure the resonator mode bandwidth in a standard way.

To verify the measurements accuracy, the resonator Q-factor was studied at a slightly different wavelength using a QCL emitting at 4.3 μm (Hamamatsu Photonics), equipped with an ultra-low-noise current driver by PPQsense. A Ge etalon (thickness 3.75 cm corresponding to 1 GHz FSR) was used as a reference [18]. The probe light was tuned through the etalon to find out tuning linearity and rate vs laser current. Fine calibration of the laser tuning was obtained by observing molecular (CO_2) Doppler-broadened transitions. The laser was tuned through the resonator mode, and the light was detected with a liquid nitrogen cooled InSb photodiode (Hamamatsu P5968-060). The resultant mode width was less than 2 MHz (FWHM) (Fig. 5), which corresponds to Q exceeding 3.5×10^7. This is exactly the number inferred from the measurement of transmission versus the air gap.

4 Conclusion

We show in this paper that measuring optical transmission through (and reflection from) a whispering gallery mode resonator allows inferring the quality factor of the resonator modes. This technique is important for the case when frequency calibration cannot be performed. We validated the applicability of the formula derived for the loading of a spherical whispering gallery mode resonator by a prism coupler to spheroidal resonators. Our validated model will allow extension of WGMRs in many fields of application, above all in molecular spectroscopy, metrology and optics throughout the huge transparency range of resonator material.

Acknowledgements The authors acknowledge financial support from Extreme Light Infrastructure (ELI) European project, from INFN under the SUPREMO project, from Ente Cassa di Risparmio di Firenze under the COSMO project.

References

1. S. Schiller, R.L. Byer, High-resolution spectroscopy of whispering gallery modes in large dielectric spheres. Opt. Lett. **16**, 1138–1140 (1991)
2. L. Collot, V. Lefevre-Seguin, M. Brune, J.M. Raimond, S. Haroche, Very high-Q whispering-gallery mode resonances observed on fused silica microspheres. Europhys. Lett. **23**, 327–329 (1993)
3. L. Gorodetsky, A.A. Savchenkov, V.S. Ilchenko, Ultimate Q of optical microsphere resonators. Opt. Lett. **21**, 453455 (1996)
4. A.A. Savchenkov, A.B. Matsko, V.S. Ilchenko, L. Maleki, Optical resonators with ten million finesse. Opt. Express **15**, 6768–6773 (2007)
5. M. Pollinger, D. OShea, F. Warken, A. Rauschenbeutel, Ultrahigh-Q tunable whispering-gallery-mode microresonator. Phys. Rev. Lett. **103**, 053901 (2009)
6. H. Tavernier, P. Salzenstein, K. Volyanskiy, Y.K. Chembo, L. Larger, Magnesium fluoride whispering gallery mode disk-resonators for microwave photonics applications. IEEE Photon. Technol. Lett. **22**, 1629–1631 (2010)
7. R.K. Chang, A.J. Campillo (eds.), *Optical Processes in Microcavities, Advanced Series in Applied Physics*, vol. 3 (World Scientific, Singapore, 1996)
8. K.J. Vahala, Optical microcavities. Nature **424**, 839–846 (2003)

9. L. Maleki, V.S. Ilchenko, A.A. Savchenkov, A.B. Matsko, Crystalline whispering gallery mode resonators in optics and photonics, chapter 3, in *Practical Applications of Microresonators in Optics and Photonics*, ed. by A.B. Matsko (CRC, Boca Raton, 2009)
10. Ivan S. Grudinin, Kamjou Mansour, Yu. Nan, Properties of fluoride microresonators for mid-IR applications. Opt. Lett. **41**, 2378 (2016)
11. M. Siciliani de Cumis, S. Borri, G. Insero, I. Galli, A. Savchenkov, D. Eliyahu, V. Ilchenko, N. Akikusa, A. Matsko, L. Maleki, P. De Natale, Microcavity-stabilized quantum cascade laser. Laser Photon. Rev. **10**, 153157 (2016)
12. C. Lecaplain, C. Javerzac-Galy, M.L. Gorodetsky, T.J. Kippenberg, Mid-infrared ultra-high-Q resonators based on fluoride crystalline materials. Nat. Commun. **7**, 13383 (2016)
13. A. Yariv, Critical coupling and its control in optical waveguide-ring resonator systems. IEEE Photon. Technol. Lett. **14**, 483–485 (2002)
14. M.L. Gorodetsky, V.S. Ilchenko, Optical microsphere resonators: optimal coupling to high-Q whispering-gallery modes. J. Opt. Soc. Am. B **16**, 147–154 (1999)
15. M. Cai, O. Painter, K.J. Vahala, Observation of critical coupling in a fiber taper to a silica-microsphere whispering-gallery mode system. Phys. Rev. Lett. **85**, 74–77 (2000)
16. S.M. Spillane, T.J. Kippenberg, O.J. Painter, K.J. Vahala, Ideality in a fiber-taper-coupled microresonator system for application to cavity quantum electrodynamics. Phys. Rev. Lett. **91**, 043902 (2003)
17. A.A. Savchenkov, W. Liang, A.B. Matsko, V.S. Ilchenko, D. Seidel, L. Maleki, Narrowband tunable photonic notch filter. Opt. Lett. **34**, 1318–1320 (2009)
18. S. Borri, M.Siciliani de Cumis, G. Insero, S. Bartalini, P.Cancio Pastor, D. Mazzotti, Iacopo Galli, G. Giusfredi, G. Santambrogio, A. Savchenkov, D. Eliyahu, V. Ilchenko, N. Akikusa, A. Matsko, L. Maleki, P. De Natale, Tunable microcavity-stabilized quantum cascade laser for mid-ir high-resolution spectroscopy and sensing. Sensors **16**, 238 (2016)